HOKKAIDO UNIVERSITY

Title	Histological alteration of bone specific-blood vessels in murine long bones with intermittent PTH administration
Author(s)	趙, 申
Degree Grantor	北海道大学
Degree Name	博士(歯学)
Dissertation Number	甲第13877号
Issue Date	2020-03-25
DOI	https://doi.org/10.14943/doctoral.k13877
Doc URL	https://hdl.handle.net/2115/94483
Type	doctoral thesis
File Information	Zhao_Shen.pdf

Hokkaido University Collection of Scholarly and Academic Papers : HUSCAP

博 士 論 文

Histological alteration of bone specific-blood vessels in murine long bones with intermittent PTH administration

（PTH 間歇投与によるマウス長管骨における骨特異的血管の組織学的変化）

令和２年３月申請

北海道大学
大学院歯学研究科口腔医学専攻

趙　申

Histological alteration of bone specific-blood vessels in murine long bones with intermittent PTH administration

Zhao Shen

Oral and Maxillofacial Surgery, Graduate School of Dental Medicine, Hokkaido University, Sapporo, Japan

Abbreviated Title: ***Blood vessels in PTH-administered bone***

[#]Address for correspondence:

Zhao Shen
Oral and Maxillofacial Surgery,
Graduate School of Dental Medicine, Hokkaido University
Kita 13 Nishi 7 Kita-ku
Sapporo, 060-8586, Japan
Tel/Fax: +81-11-706-4283
E-mail: zhaoshen@den.hokudai.ac.jp

Abstract

It is well known that the intermittent administration of parathyroid hormone (PTH) promotes bone formation, but it remains to be unveiled if PTH could affect the distribution of bone-specific blood vessels and other cell-types surrounding the blood vessels. In this study, we have attempted to histologically examine bone-specific blood vessels after intermittent PTH administration. Six-week-old C57BL/6J mice received vehicle (control group) or 20 μg/kg/day of hPTH [1–34] (PTH group) for two weeks. The mice were then fixed and their femora and tibiae were examined for the immunohistochemical profile. The gene expression of bone was also examined by RT-PCR. In the control femoral metaphysis, there were many endomucin-positive/EphB4-positive blood vessels and few αSMA-reactive blood vessels. In the PTH administered femoral metaphysis, the numbers of endomucin-positive/EphB4-positive blood vessels and their diameters were significantly expanded when compared to those of the control groups. Interestingly, blood vessels accompanied with αSMA-positive cells were significantly increased in number in the PTH group, and were histochemically divided into two distinct types: the one surrounded by ALP-reactive/αSMA-positive cells close to the bone surface, and the others accompanied merely with αSMA-positive cells that showed a long cell shape extending thin cytoplasmic processes. In summary, the intermittent administration of PTH may affect both osteoblastic cells and bone-specific blood vessels.

210 words

Keywords: *blood vessel, bone, parathyroid hormone (PTH), endomucin, vascular smooth muscle cell*

Introduction

Osteoporosis is a typical symptom in geriatric disease. For years, the first-line drug in therapy for osteoporosis has remained bisphosphonates [1]. However, it has been reported that bisphosphonates could be associated with severe complications such as osteonecrosis of the jaw or atypical femur fractures [2]. Over the last decade, teriparatide, which is a recombinant form of parathyroid hormone (PTH), has become the preferred drug for the treatment of osteoporosis [1, 3]. The anabolic action of PTH has also been demonstrated in clinical trials: PTH increased bone mass and reduced the fracture rate in patients with osteoporosis [4]. In our previous study, we have demonstrated that intermittent PTH administration promotes preosteoblastic proliferation and osteoblastic bone formation, both of which are finely tuned by cell coupling with osteoclasts, and finally induced new bone formation [5, 6].

Recently, Kusumbe and Ramasamy demonstrated two new disparate subtypes of endothelial cells in bone according to distribution and function: type H and type L [7]. The type H bone-specific subtype is a blood vessel that features CD31 and endomucin double strong positivity located underneath the growth plate in the metaphysis, while the type L subtype showed CD31 and endomucin low positivity in diaphysis [7, 8]. Endomucin^{high}-positive bone-specific blood vessels have been shown to reciprocally interact with osteoblastic cells [7]. Endomucin^{high}-positive endothelial cells have been reported to secrete noggin, supporting osteoblasts and chondrocytes, which secrete vascular endothelial growth factor (VEGF) sustaining angiogenesis in reverse [7, 8]. This may implicate the reciprocal interaction of blood vessels and osteoblastic cells in bone in a normal state.

It is well-known that blood vessels consist of various cell-types, being roughly divided into inner vascular endothelial cells and outer perivascular cells [9]. A vascular smooth muscle cell is a type of perivascular cell that always covers arteries/veins including arterioles and venules and appears to regulate vessel caliber [10]. α-Smooth muscle actin (αSMA) is a specific marker of vascular smooth muscle cells and myofibroblasts [11]. The nutrient arteries and arterioles surrounded by vascular smooth muscle cells invade from the periosteum into the bone and run in the inner bone marrow region of the diaphyses of long bones [12]. However, the peripheral vascular smooth muscle cells gradually disappear to form sinusoidal capillaries that extend from the sinusoidal capillaries toward the chondro-osseous

junctions, where they are not covered by peripheral vascular smooth muscle cells and are sometimes surrounded by discontinuous basement membranes [10]. Therefore, perivascular cells including vascular smooth muscle cells will not always be adjacent to vascular endothelial cells, depending on the micro-circumstance of the blood vessels. It is assumed that perivascular cells such as vascular smooth muscle cells may not be fully differentiated but still possess the potential to differentiate into other cell types [10, 11, 13]. Indeed, it has been reported that arteries in bone are covered by αSMA-positive smooth muscle cells that have the potential to differentiate into different mesenchymal lineages [14–16].

Recently, considerable reports have supported the importance of the interactions between EphB4 and ephrinB2 in the cardiovascular system and skeletal system [17, 18]. EphB4 is a marker for veins, while ephrinB2 is a marker for arteries. Since previous reports have suggested EphB4/ephrinB2 action as a coupling factor in bone [17], it may be possible for EphB4-positive veins/ephrinB2-reactive arteries to affect the activities of osteoblastic cells. Thus, PTH-driven anabolic effects may affect both osteoblastic cells and vascular endothelial cells and the surrounding perivascular cells including vascular smooth muscle cells. Alternately, it might be possible that PTH would directly affect vascular endothelial cells of bone-specific blood vessels and surrounding vascular smooth muscle cells. However, the biological effects of PTH on bone-specific blood vessels including vascular endothelial cells and surrounding vascular smooth muscle cells remain unknown.

Therefore, in this study we have attempted to histochemically examine the bone-specific blood vessels in long bone after intermittent PTH administration *in vivo*.

Materials and methods

Animals

Six-week-old male C57BL/6J mice (n = 12, Japan CLEA, Tokyo, Japan) were divided into a control group and PTH group following the principles for animal care and research use set by Hokkaido University (approved No: 15-0032). The control group received vehicle (0.9% saline) while the PTH group received hPTH [1–34] (Sigma-Aldrich Co., LLC., St. Louis, MO). According to our previous report [6], the mice received 20 μg/kg/day of hPTH [1–34] twice per day. Intraperitoneal injections were performed at 8:00 am and 8:00 pm for two weeks. Mice were kept under standard conditions.

Specimen preparation

Before fixation, mice were anesthetized with an intraperitoneal injection of chloral hydrate for bodyweight determination. Then, all mice were perfused with 4% paraformaldehyde diluted in 0.1 M cacodylate buffer (pH 7.4) through the cardiac left ventricle. After perfusion with 4% paraformaldehyde solution, the femora and tibiae were extracted promptly and immersed in the same solution for 24 hours at 4°C. After washing in phosphate-buffered saline (PBS) for three days, all the samples were decalcified with 10% or 4.13% EDTA-2Na for paraffin-specimens and epoxy resin-specimens, respectively. For paraffin-embedded specimens, samples were dehydrated in ascending ethanol solutions, soaked in xylene, and finally embedded in paraffin. For epoxy resin-embedded specimens, samples were post-fixed with 1% osmium tetraoxide in a 0.1 M cacodylate buffer for eight hours at 4°C, dehydrated in ascending acetone solutions, and finally embedded with epoxy resin (Epon 812).

Histological and immunohistochemical detection

Dewaxed paraffin sections were examined for endomucin, αSMA, EphB4 and ephrin B2 as previously examined [5]. The sections were treated for endogenous peroxidase inhibition with 0.3% H_2O_2 in PBS for 30 mins, and subsequently for nonspecific staining blocking by 1% bovine serum albumin (BSA; Serologicals Proteins Inc. Kankakee, IL) in PBS (1% BSA-PBS) for 20 mins at room temperature. Then, sections were incubated with rat antibody against endomucin (Santa Cruz Biotechnology, Inc., Dallas, TX) at a dilution of 1:100 and 4°C overnight. Following

several washings in PBS, they were incubated with horseradish peroxidase (HRP)-conjugated anti-rat IgG (Zymed Laboratories Inc., South San Francisco, CA) at a dilution of 1:100. To detect αSMA, the dewaxed sections treated with 1% BSA–PBS were incubated with mouse antibody against αSMA (Thermo Fisher Scientific Inc., Cheshire, UK) at a dilution of 1:400 and 4°C overnight. Then, the sections were incubated with HRP-conjugated rabbit anti-mouse IgG (Bethyl Laboratories, Inc., Montgomery, TX). For the detection of EphB4 and ephrinB2, the dewaxed sections were reacted with goat antibody against mouse EphB4 (R&D Systems Inc., Minneapolis, MN) at a dilution of 1:50 or with goat antibody against mouse ephrinB2 (R&D Systems Inc., Minneapolis, MN) at a dilution of 1:50 and 4°C overnight. After several washings in PBS, they were incubated with HRP-conjugated rabbit anti-goat IgG (American Qualex Scientific Products, Inc., San Clemente, CA) for 1 h. Immune complexes of all sections were visualized using 3, 3'-diaminobenzidine tetrahydrochloride (Dojindo Laboratories, Kumamoto, Japan). Then, specimens were observed under a Nikon Eclipse Ni microscope (Nikon Instruments Inc. Tokyo, Japan), and light microscopic images were acquired with a digital camera (Nikon DXM1200C, Nikon).

Double immunohistochemical and immunofluorescence staining

For αSMA/endomucin double immunohistochemical staining procedures, dewaxed paraffin sections were incubated with 1% BSA–PBS and then with mouse antibody against αSMA (Thermo Fisher Scientific Inc.) at a dilution of 1:400 with 1% BSA–PBS. After that, they were incubated with fluorescein (FITC)-conjugated goat anti-mouse IgG (MP Biomedicals. LLC., Solon, OH) at a dilution of 1:100 with 1% BSA–PBS and then incubated with rat antibody against endomucin at a dilution of 1:100 at 4°C after washing with PBS. Sections were subsequently reacted with Alexa 594-conjugated rabbit anti-rat IgG (Thermo Fisher Scientific Inc., Cheshire, UK) at a dilution of 1: 100. For the detection of αSMA and ALP, dewaxed paraffin sections were incubated with 1% BSA–PBS and then with mouse antibody against αSMA (Thermo Fisher Scientific Inc.) at a dilution of 1:400 with 1% BSA–PBS; then, they were incubated with fluorescein (FITC)-conjugated goat anti-mouse IgG (MP Biomedicals. LLC., Solon, OH) at a dilution of 1:100. After PBS washing, the sections were reacted with rabbit polyclonal antisera against TNALP at a dilution of 1:300 with 1% BSA–PBS; then, they were incubated with Alexa Fluor

594-conjugated goat anti-rabbit IgG (Thermo Fisher Scientific, Inc, Waltham, MA) at a dilution of 1:100 with 1% BSA–PBS for 1 h. All sections were embedded by VECTASHIELD hard-set mounting medium with DAPI (Vector Laboratories, Inc. Burlingame, CA) and observed under light microscopy.

Toluidine blue staining

Semi-thin sections were prepared with an ultramicrotome and were then stained with toluidine blue staining and observed under a Nikon microscope. Light microscopy images were acquired with a digital camera.

Static parameters for bone histomorphometry

A 800×1000 μm Region of Interest (ROI) located underneath the growth plate of femoral metaphysis was employed to assess the following static parameters: number of endomucin-positive, αSMA-positive, EphB4-positive, and ephrinB2-positive blood vessels, maximum diameter (length of longest line joining two points of blood vessel's outline and passing through the centroid)/minimum diameter (length of the shortest line joining two points in the blood vessel's outline and passing through the centroid)/mean diameter (average length of diameters measured at 2 degree intervals and passing through the blood vessel's centroid) of the endomucin-immunopositive blood vessels, area of the endomucin-reactive blood vessels. Images of the ROI stained for endomucin/αSMA, EphB4, ephrinB2 from the control groups and PTH groups (n = 6 for each group) were used to determine the number of each kind of vessel and the external diameter of the endomucin-immunoreactive blood vessel within the ROI were measured with Image-Pro Plus 6.2 (Media Cybernetics, Inc., Bethesda MD); the results were later statistically analyzed as follows.

RT-PCR assessment

Total RNA was extracted from fresh frozen femora and tibiae using TRIzol reagent (Life Technologies Co., Carlsbad, CA). For RT-PCR, total RNA was reverse transcribed to cDNA using SuperScript VILO cDNA Synthesis Kit (Life Technologies). For PCR amplification, the following primer sets were used: (forward) 5′- TGTCTTCACCACCATGGAGAAGG -3′ and (reverse) 5′- GTGGATGCAGGGATGATGTTCTG -3′ for GAPDH, (forward) 5′- CTATGAAAATAACAGTGCCAAATACTCCAA -3′ and (reverse) 5′-

AGGATCCATCACGATGTCAGTTCTTGGTTT -3′ for endomucin, and (forward) 5′-GTATGTGGCTATTCAGGCTG -3′ and (reverse) 5′-CTTCTGCATCCTGTCAGCAA -3′ for α-SMA, (forward) 5′-CCCAAATAGGAGACGAGTCC -3′ and (reverse) 5′-CTCAAAAGGAGGTGGTCCAG -3′ for EphB4, and (forward) 5′-TCCAGGAGGGACTCTGTGTGGAAG -3′ and (reverse) 5′-CGGGGTATTCTCCTTCTTAATTGT -3′ for ephrinB2. PCR products were electrophoresed on a 2% agarose gel containing ethidium bromide and visualized with UV light.

Statistical analysis

All statistical analyses were carried out using SPSS version 18.0.0 and analyzed for statistical significance by Student's t-test. Data values were presented as mean ± SE. For the study, any p-value of 0.05 was considered statistically significant.

Results

Altered distribution of bone specific-blood vessels after intermittent PTH administration

Metaphyseal trabeculae and the trabecular bone mass were increased in femora of the PTH group compared with the control group **(Figure 1A–B)**. After PTH administration, the number of endomucin-positive blood vessels appeared to increase histologically and their diameters seemed to expand compared to the control groups **(Figure 1C–D)**. Therefore, we measured the cross-sectioned maximum diameter, the minimum diameter, and the mean diameter of the endomucin-reactive blood vessels in the ROI of 800 μm x 1,000 μm **(Figure 1E)**. One consequence of intermittent PTH administration is that the indices of the maximum and mean diameter of the endomucin-immunoreactive blood vessels were significantly higher than those of the control specimens. The average maximum diameter of the endomucin-immunoreactive blood vessels in the control group were 224.53 ± 10.06 μm and the average mean diameter of the endomucin-reactive blood vessels was 121.37 ± 4.76 μm. In the PTH group, the average maximum diameter and mean diameter of the endomucin-reactive blood vessels were 339.22 ± 14.58 μm ($p < 0.01$ vs. control) and 144.01 ± 4.63 μm ($p < 0.05$ vs. control), respectively. There was no significant difference in the minimum diameter of the endomucin-positive blood vessels between the control group and the PTH group as shown in **Figure 1E**. The average minimum diameter of the endomucin-reactive blood vessels was 73.16 ± 2.94 μm in the control group and 73.26 ± 2.32 μm in the PTH group. Additionally, we examined the cross-section areas of the endomucin-immunopositive blood vessels in the ROI **(Figure 1F)**. After intermittent PTH administration, the area of the endomucin-reactive blood vessels had significantly increased: The cross-sectioned areas of the endomucin-immunopositive blood vessels were 19,841.02 ± 2,585.61 μm^2 in the control group and 28,652.31 ± 2,413.11 μm^2 in the PTH group ($p < 0.05$).

Immunolocalization of αSMA-immunoreactive, EphB4-immunoreactive and ephrinB2-immunoreactive cells in PTH-administrated blood vessels

The number of αSMA-immunopositive cells was markedly-increased in the vicinity of endomucin-reactive blood vessels after PTH administration. There was a huge number of αSMA-reactive blood vessels in the metaphyses by PTH administration,

while there seemed a few αSMA-positive blood vessels in the control counterparts **(Figure 2A–C)**. In addition, the numbers of EphB4-positive blood vessels and ephrinB2-positive arteries increased in PTH-treated metaphyses when compared with those in the control specimens **(Figure 2 D–I)**.

Using the immunostained sections, we counted the number of each type of blood vessel in the ROI underneath the growth plate. After intermittent PTH administration, the numbers of endomucin-positive, αSMA-positive, EphB4-positive, and ephrinB2-positive blood vessels were significantly increased **(Figure 2J)**. The numbers of endomucin-positive, αSMA-positive, EphB4-positive, and ephrinB2-positive blood vessels in the control group were 50.17 $\pm$ 18.45, 3.50 $\pm$ 2.17, 63.00 $\pm$ 18.01, and 4.00 $\pm$ 1.55, respectively. The numbers of endomucin-positive, αSMA-positive, EphB4-positive, and ephrinB2-positive blood vessels in the PTH group were 82.33 $\pm$ 14.63, 26.67 $\pm$ 7.58, 147 $\pm$ 42.37, and 21.5 $\pm$ 4.84, respectively ($p < 0.01$ vs. control). When examined by RT-PCR, the gene expressions of endomucin, αSMA, EphB4, and ephrinB2 in the femora consistently appeared elevated after PTH administration **(Figure 2K)**.

The distribution of αSMA-immunoreactive cells surrounding endomucin-immunoreactive blood vessels in PTH-administered metaphyses

Some αSMA-immunopositive cells seemed closely associated with endomucin-positive vascular endothelial cells, being identical to vascular smooth muscle cells. However, the others were located somewhat apart from the blood vessels, and therefore appeared to be cell-types other than vascular smooth muscle cells **(Figure 3A–D)**. To define the characteristics of αSMA-positive cells not identical to vascular smooth muscle cells, we examined the double immunodetection of ALP and αSMA, and consequently divided them into two distinct cell-types **(Figure 3E–H)**: the αSMA-positive cells bearing ALP-reactivity located in close proximity to the blood vessels in the intertrabecular regions **(Figure 3E and G)**, and the αSMA-positive but ALP-negative cells that extend long cell bodies and thin cytoplasmic processes **(Figure 3F and H)**. Taken together, three αSMA-positive cell-types appeared after PTH administration: αSMA-positive vascular smooth muscle cells, αSMA/ALP double-positive cells close but not adjacent to blood vessels, and αSMA-positive/ALP-negative cells that extend their straightly extending cytoplasmic processes. Thus, it appears that the cellular population surrounding the

blood vessels changes after PTH administration. Therefore, we examined the corresponding region using semi-thin sections **(Figure 4)**. Two distinct cell-types were shown to be located around blood vessels in the femoral metaphysis of the PTH-administered mice **(Figure 4B–D)**. One was the cells revealing a long cell-shape with thin cytoplasmic processes distant from bone, and the other was the cells containing several cell organelles in the somehow translucent cytoplasm.

Discussion

In this study, we have attempted to histologically demonstrate the altered distribution of bone-specific blood vessels in murine bone after intermittent PTH administration. Our main histological findings can be summarized as follows:

1) Intermittent PTH administration increased the number of endomucin-positive blood vessels and significantly expanded their diameter.

2) The numbers of αSMA-positive, ephrinB2-positive, and EphB4-positive blood vessels also increased after PTH administration.

3) αSMA-positive cells were markedly-increased in number and can be distinctively divided into the first type, αSMA-positive vascular smooth muscle cells closely surrounding the endomucin-reactive vascular endothelial cells, the second type, αSMA/ALP double-positive cells close but not adjacent to blood vessels, and the third type, αSMA-positive but ALP-negative cells extending their straightly extending cytoplasmic processes.

To our knowledge, this is the first report to suggest that the intermittent administration of PTH affects bone-specific blood vessels in bone.

One may wonder why we have employed regimens of two- and four-times administration of PTH each day. Using murine models, we have recently demonstrated that the high frequency of intermittent PTH administration (two or four times per day) promotes bone remodeling by stimulating both bone resorption and formation, while low-frequency PTH administration (once a day or per two days) caused both remodeling-based/mini-modeling-based bone formation [6]. In addition, we have reported that high-frequency PTH administration stimulated preosteoblastic proliferation and subsequent osteoblastic differentiation by mediating cell coupling with osteoclasts [5]. Therefore, the anabolic effects of PTH appear to be based on accelerated preosteoblastic proliferation and finely-tuned cell coupling with osteoclasts.

These cellular events take place in the region of mature osteoblasts including preosteoblastic cells, bone marrow-stromal cells, and blood vessels rather than in the region of the osteocytic network embedded in bone, although many investigators have suggested that PTH-driven anabolic action is reportedly mediated by the sclerostin/Wnt pathway of osteocytes [21, 22]. In accordance with our previous

reports, we decided to employ high-frequency PTH administration in this study rather than low-frequency to ensure adequate regimens to examine the bone specific-blood vessels and the surrounding cells; consequently, we were able to observe the significant alteration of bone specific-blood vessels by PTH.

Regarding the biological actions of blood vessels in bone, many studies have paid close attention to the intimate connection between blood vessels and bone tissues [23]. Since bone is highly vascularized tissue, it has been previously assumed that blood vessels serve as a tunnel by which to transmit oxygen, nutrition, growth factors, and hormones into the bone and take part in the hematopoiesis of neighboring bone marrow [9]. Recently, it has been demonstrated that there is a network of trans-cortical capillaries as a mainstay for blood circulation in long bone [24]. Literally, Kusumbe and Ramasamy et al. reported a bone-specific subtype of blood vessels featuring $CD31^{high}$/$endomucin^{high}$, and illuminated that angiogenesis also plays an important role in bone development and remodeling [7, 8]. $Endomucin^{high}$-positive blood vessels in the metaphyses of long bone have been shown to reciprocally interact with osteoblastic cells requiring various cytokines, microRNA, and signaling pathways. Thus, while recent studies on bone/blood vessel interaction have progressed, few reports have elucidated the biological action of PTH on bone-specific blood vessels.

In the present study, intermittent PTH administration increased the number of endomucin-immunoreactive/EphB4-positive blood vessels and the maximum/mean diameters and area of endomucin-positive blood vessels in the metaphyses of murine femora and tibiae. Since most blood vessels in this area are capillaries that are not surrounded by vascular smooth muscle cells, the enlargement of blood vessels in this area seems non-ascribable to the relaxation of vascular smooth muscle cells but is rather probably due to morphological changes in the capillaries. In addition, we assume that the reason why blood vessels increased in number might be due to angiogenesis stimulated by PTH. Another interpretation may be that PTH mainly reacts to the development and remodeling of bone by the classical Wnt/β-catenin pathway [22], which might be able to react to the angiogenesis by the VEGF-relevant pathway. However, further investigation is necessary to define the cellular mechanism of the increased numbers and diameters of capillaries after PTH administration.

We have observed that three αSMA-positive cell-types appear after PTH administration: the first is αSMA-positive vascular smooth muscle cells closely

surrounding the endomucin-reactive vascular endothelial cells, the second is αSMA/ALP double-positive cells close but not adjacent to blood vessels, and the third is αSMA-positive but ALP-negative cells extending their straightly extending cytoplasmic processes. The first appears to be vascular smooth muscle cells, but the other two might be other cell-types. Since the control vascular endothelial cells were hardly accompanied by αSMA-positive vascular smooth muscle cells in the metaphyses, it seems likely that undifferentiated perivascular cells might differentiate into vascular smooth muscle cells by PTH administration. αSMA-positive/ALP-reactive cells that were located close but not adjacent to endomucin-positive/αSMA-reactive blood vessels seem different to vascular smooth muscle cells even though they showed αSMA-immunoreactivity. It has been previously reported that arteries in bone were covered by αSMA-positive/NG2-reactive vascular smooth muscle cells [14], possessing the potential to differentiate into other mesenchymal lineages [7, 8]. Therefore, αSMA-positive/ALP-reactive cells close to the blood vessels might be derived from vascular smooth muscle cells that have differentiated from perivascular cells. Alternately, perivascular cells may have directly differentiated into αSMA-positive/ALP-reactive cells. A previous study indicated that PTH may promote vascularized bone regeneration and directly improve blood vessel formation and the osteogenic potential of aged bone marrow mesenchymal stem cells [25]. Since ALP is an important bone metabolic marker expressed in the osteoblastic lineage [26–28] that also comes from bone marrow mesenchymal cells, these cells may be able to differentiate into preosteoblasts/osteoblasts. Taken together, it may be possible for PTH to stimulate perivascular cells to differentiate into either vascular smooth muscle cells or an ALP-positive osteoblastic lineage.

Regarding αSMA-positive/ALP-negative cells with long cell bodies and thin cytoplasmic processes located in middle of the intertrabecular region, this cell-type extends long cytoplasmic processes linearly parallel to the bone surface. Judging from the cell shape and long cytoplasmic processes, this may be a kind of telocyte that was discovered in 2003 [29]. Telocytes are fibroblast-like cells extending extremely long but thin prolongations. There has not yet been any report of the discovery of telocytes in bone and further examination is warranted. Taken together, bone specific-blood vessels may play an important role in the bone formation process.

In summary, the intermittent administration of PTH may affect both osteoblastic

cells and bone-specific blood vessels.

References

1. Schweser KM, Crist BD (2017) Osteoporosis: a discussion on the past 5 years. Curr Rev Musculoskelet Med 10: 265–274

2. Kim SC, Kim DH, Mogun H, Eddings W, Polinski JM, Franklin JM Solomon DH (2016) Impact of the U.S. food and drug administrations safety-related announcements on the use of bisphosphonates after hip fracture. J Bone Miner Res 31: 1536–1540

3. Orwoll E, Scheele W, Paul S, Adami S, Syversen U, Diez-Perez A, Kaufman JM, Clancy AD, Gaich GA (2003) The effect of teriparatide [human parathyroid hormone (1–34)] therapy on bone density in men with osteoporosis. J Bone Miner Res 18: 9–17

4. Skripitz R, Aspenberg P (2004) Parathyroid hormone--a drug for orthopedic surgery? Acta Orthop Scand 75: 654–662

5. Luiz de Freitas PH, Li M, Ninomiya T, Nakamura M, Ubaidus S, Oda K, Udagawa N, Maeda T, Takagi R, Amizuka N (2009) Intermittent PTH administration stimulates pre-osteoblastic proliferation without leading to enhanced bone formation in osteoclast-less c-fos(-/-) mice. J Bone Miner Res 24: 1586–1597

6. Yamamoto T, Hasegawa T, Sasaki M, Hongo H, Tsuboi K, Shimizu T, Ohta M, Haraguchi M, Takahata T, Oda K, Freitas PHL, Takakura A, Takao-Kawabata R, Isogai Y, Amizuka N (2016) Frequency of teriparatide administration affects the histological pattern of bone formation in young adult male mice. Endocrinology 157: 2604–2620

7. Kusumbe AP, Ramasamy SK, Adams RH (2014) Coupling of angiogenesis and osteogenesis by a specific vessel subtype in bone. Nature 507: 323–328

8. Ramasamy SK, Kusumbe AP, Wang L, Adams RH (2014) Endothelial Notch activity promotes angiogenesis and osteogenesis in bone. Nature 507: 376–380

9. Sivaraj KK, Adams RH (2016) Blood vessel formation and function in bone. Development 143: 2706–2715

10. Armulik A, Genove G, Betsholtz C (2011) Pericytes: developmental, physiological, and pathological perspectives, problems, and promises. Dev Cell 21: 193–215

11. Aizman I, Holland WS, Yang C, Bates D (2016) alphaSMA Expression in Large Colonies of Colony-Forming Units-Fibroblast as an Early Predictor of Bone Marrow MSC Expandability. Cell Med 8: 79–85

12. Ramasamy SK (2017) Structure and functions of blood vessels and vascular niches in bone. Stem Cells Int 2017: 5046953

13. Matthews BG, Grcevic D, Wang L, Hagiwara Y, Roguljic H, Joshi P, Shin DG, Adams DJ, Kalajzic I (2014) Analysis of alphaSMA-labeled progenitor cell commitment identifies notch signaling as an important pathway in fracture healing. J Bone Miner Res 29: 1283–1294

14. Kusumbe AP, Ramasamy SK, Itkin T, Mae MA, Langen UH, Betsholtz C, Lapidot T, Adams RH (2016) Age-dependent modulation of vascular niches for haematopoietic stem cells. Nature 532: 380–384

15. Kunisaki Y, Bruns I, Scheiermann C, Ahmed J, Pinho S, Zhang D, Mizoguchi T, Wei Q, Lucas D, Ito K, Mar JC, Bergman A, Frenette PS (2013) Arteriolar niches maintain haematopoietic stem cell quiescence. Nature 502: 637–643

16. Mendez-Ferrer S, Michurina TV, Ferraro F, Mazloom AR, Macarthur BD, Lira SA, Scadden DT, Maayan A, Enikolopov GN, Frenette PS (2010) Mesenchymal and haematopoietic stem cells form a unique bone marrow niche. Nature 466: 829–834

17. Rundle CH, Xing W, Lau KW, Mohan S (2016) Bidirectional ephrin signaling in bone. Osteoporos Sarcopenia 2: 65–76

18. Zhao C, Irie N, Takada Y, Shimoda K, Miyamoto T, Nishiwaki T, Suda T, Matsuo K (2006) Bidirectional ephrinB2-EphB4 signaling controls bone homeostasis. Cell Metab 4: 111–121

19. Ng YS, Ramsauer M, Loureiro RM, DAmore PA (2004) Identification of genes involved in VEGF-mediated vascular morphogenesis using embryonic stem cell-derived cystic embryoid bodies. Lab Invest 84: 1209–1218

20. Allan EH, Hausler KD, Wei T, Gooi JH, Quinn JM, Crimeen-Irwin B, Pompolo S, Sims NA, Gillespie MT, Onyia JE, Martin TJ (2008) EphrinB2 regulation by PTH and PTHrP revealed by molecular profiling in differentiating osteoblasts. J Bone Miner Res 23: 1170–1181

21. Du JH, Lin SX, Wu XL, Yang SM, Cao LY, Zheng A, Wu JN, Jiang XQ (2019) The function of Wnt ligands on osteocyte and bone remodeling. J Dent Res 98:

930–938.

22. Baron R, Hesse E (2012) Update on bone anabolics in osteoporosis treatment: rationale, current status, and perspectives. J Clin Endocrinol Metab 97: 311–325

23. Portal-Nunez S, Lozano D, Esbrit P (2012) Role of angiogenesis on bone formation. Histol Histopathol 27: 559–566

24. Grüneboom A, Hawwari I, Weidner D, Culemann S, Müller S, Henneberg S, Henneberg S, Brenzel A, Merz S, Bornemann L, Zec K, Wuelling M, Kling L, Hasenberg M, Voortmann S, Lang S, Baum W, Ohs A, Kraff O, Quick HH, Jäger M, Landgraeber S, Dudda M, Danuser R, Stein JV, Rohde M, Gelse K, Garbe AI, Adamczyk A, Westendorf AM, Hoffmann D, Christiansen S, Engel DR, Vortkamp A, Krönke G, Herrmann M, Kamradt T, Schett G, Hasenberg A, Gunzer M (2019) A network of trans-cortical capillaries as mainstay for blood circulation in long bones. Nature Metabolism 1:236–250

25. Jiang L, Zhang W, Wei L, Zhou Q, Yang G, Qian N, Tang Y, Gao Y, Jiang X (2018) Early effects of parathyroid hormone on vascularized bone regeneration and implant osseointegration in aged rats. Biomaterials 179:15–28

26. Rey A, Manen D, Rizzoli R, Ferrari SL, Caverzasio J (2007) Evidences for a role of p38 MAP kinase in the stimulation of alkaline phosphatase and matrix mineralization induced by parathyroid hormone in osteoblastic cells. Bone 41: 59–67

27. Nakajima A, Shimoji N, Shiomi K, Shimizu S, Moriya H, Einhorn TA, Yamazaki M (2002) Mechanisms for the enhancement of fracture healing in rats treated with intermittent low-dose human parathyroid hormone (1-34). J Bone Miner Res 17: 2038–2047

28. Hirota S, Takaoka K, Hashimoto J, Nakase T, Takemura T, Morii E, Fukuyama A, Morihana K, Kitamura Y, Nomura S (1994) Expression of mRNA of murine bone-related proteins in ectopic bone induced by murine bone morphogenetic protein-4. Cell and tissue research 277: 27–32

29. Marini M, Rosa I, Ibba-Manneschi L, Manetti M (2018) Telocytes in skeletal, cardiac and smooth muscle interstitium: morphological and functional aspects. Histol Histopathol 33:1151–1165

Figure legends

Fig. 1 HE staining of the control mice's femora (A) and PTH-administered mice's femora (B). The bone mass increased in the PTH-administered mice (B) compared to the control groups (A). In the metaphysis of the femora, the diameter of the endomucin-positive blood vessels (brown color) tended to expand in PTH mice (D) compared to control mice (C). Graph E showed the index of the luminal diameter of endomucin-positive blood vessels. After PTH administration, the maximum and mean diameter of the endomucin-positive blood vessels were significantly increased compared to the control group (* $p < 0.05$, ** $p < 0.01$). Graph F demonstrated the total areas of the endomucin-positive blood vessels in the ROI. The area of the endomucin-positive blood vessels was significantly expanded after PTH injection ($p < 0.05$). Bars: A, B: 500 μm C, D: 200 μm

Fig. 2 In the metaphysis, both αSMA-positive blood vessels (brown color) and αSMA-immunopositive cells close to the endomucin-reactive blood vessels tended to increase in PTH-administered groups (B and C) compared to the control group (A). Figures D–F demonstrated the immunolocalization of EphB4 (brown color) and Figures G–I showed the immunolocalization of ephrinB2 (brown color) in the control and PTH-administered groups. The number of endomucin-, αSMA-, EphB4-, and ephrinB2-positive blood vessels were significantly increased in PTH mice, respectively (J, $p < 0.01$). The gene expressions of *Endomucin*, *α-sma, Ephrinb2*, and *Ephb4* were also increased by RT-PCR analysis (K). BV: blood vessel
Bars: A, B: 200 μm C–I: 50 μm

Fig. 3 After PTH administration, αSMA-immunoreactivity (brown color: A and B; green color: C and D) were localized on the vascular smooth muscle cells associated with endomucin-positive vascular endothelial cells and other types of cells other than the blood vessels (arrows: B and D). ALP (blue color: E and F; red color: G and H) and αSMA (brown color: E and F; green color: G and H) double staining demonstrated 1) ALP-positive/αSMA-positive cells close to the blood vessels (G), and 2) ALP-negative/αSMA-positive cells extending long cell bodies and thin cytoplasmic

processes in the PTH-administered groups (arrows, H). BV: blood vessel
Bars: A, B: 200 µm C–I: 50 µm

Fig. 4 The semi-thin section obtained from the PTH group demonstrated two different type of cells in the bone marrow region over the osteoblasts (C–D). One is the spindle cell that reveals a long shape with thin cytoplasmic processes distant from the bone (inset, D), and the other is cuboidal cells that appeared to contain several cell organelles (arrows, D). ob: osteoblast; BV: blood vessel.
Bars: A, B: 50 µm C, D: 20 µm

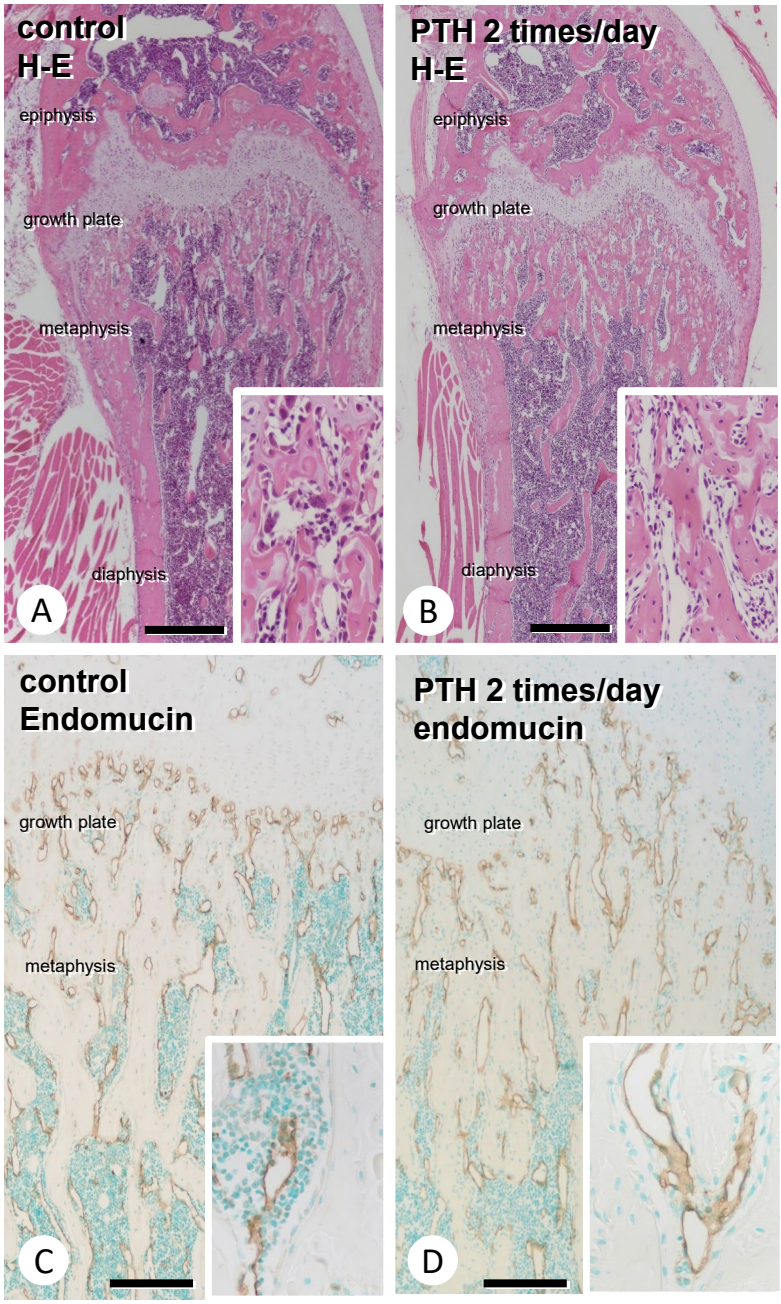
control
H-E
epiphysis
growth plate
metaphysis
diaphysis
A
PTH 2 times/day
H-E
epiphysis
growth plate
metaphysis
diaphysis
B
control
Endomucin
growth plate
metaphysis
C
PTH 2 times/day
endomucin
growth plate
metaphysis
D

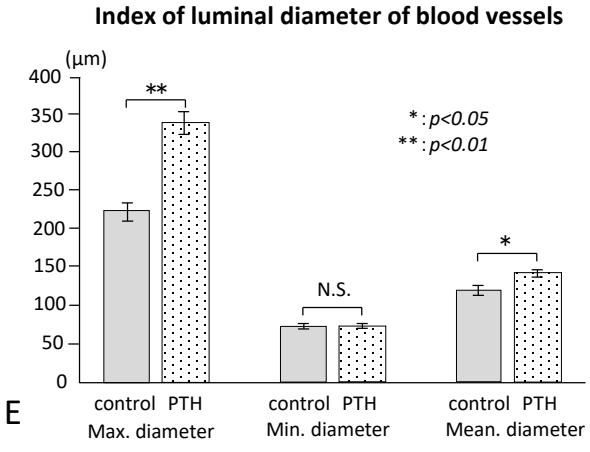
Index of luminal diameter of blood vessels
(μm)
400
350
300
250
200
150
100
50
0
**
N.S.
*
*: p<0.05
**: p<0.01
control PTH
Max. diameter
control PTH
Min. diameter
control PTH
Mean. diameter
E

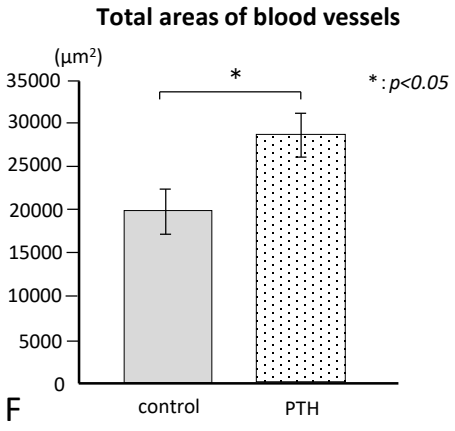
Total areas of blood vessels
(μm²)
35000
30000
25000
20000
15000
10000
5000
0
*
*: p<0.05
control
PTH
F

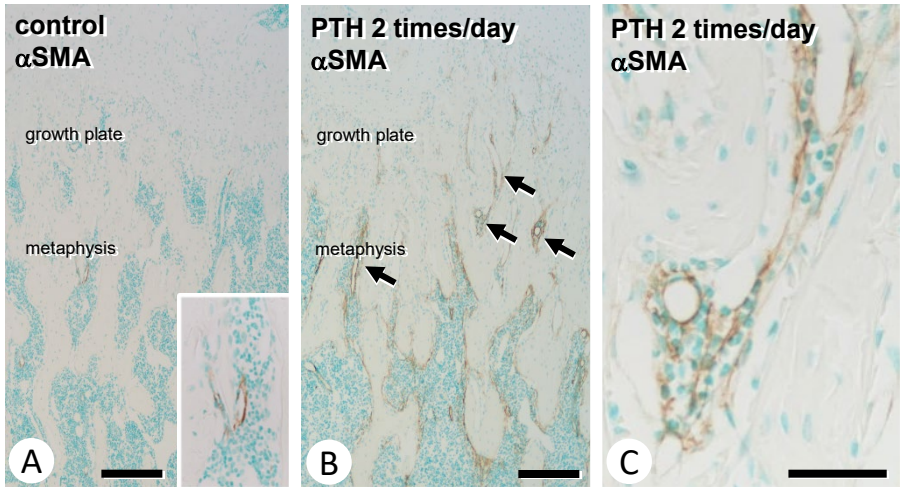
control
αSMA
growth plate
metaphysis
A
PTH 2 times/day
αSMA
growth plate
metaphysis
B
PTH 2 times/day
αSMA
C

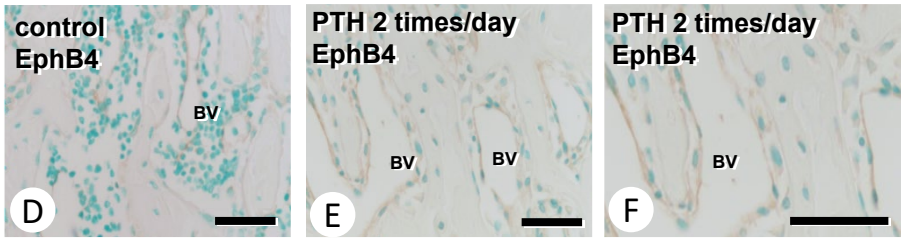
control
EphB4
BV
D
PTH 2 times/day
EphB4
BV
BV
E
PTH 2 times/day
EphB4
BV
F

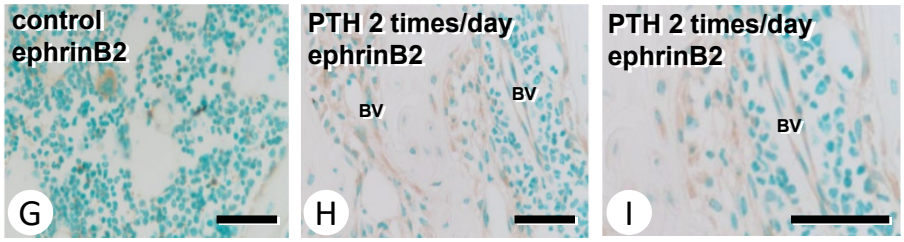
control
ephrinB2
G
PTH 2 times/day
ephrinB2
BV
BV
H
PTH 2 times/day
ephrinB2
BV
I

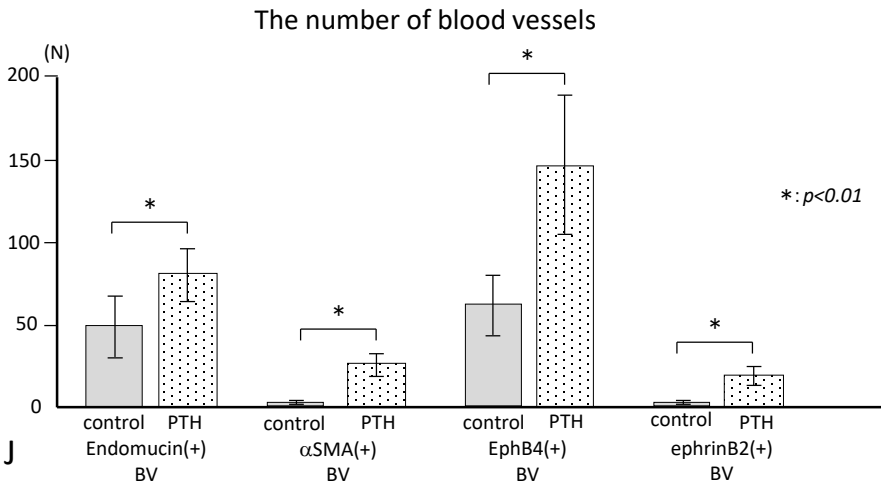
The number of blood vessels
(N)
200
150
100
50
0
*
*
*
*
*: p<0.01
control
PTH
Endomucin(+)
BV
control
PTH
αSMA(+)
BV
control
PTH
EphB4(+)
BV
control
PTH
ephrinB2(+)
BV
J

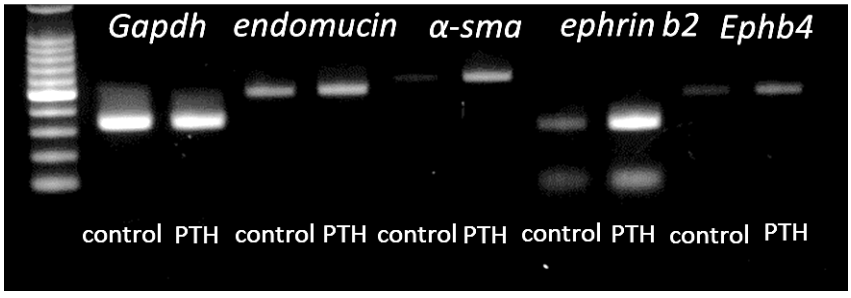
Gapdh
endomucin
α-sma
ephrin b2
Ephb4
control
PTH
control
PTH
control
PTH
control
PTH
control
PTH
K

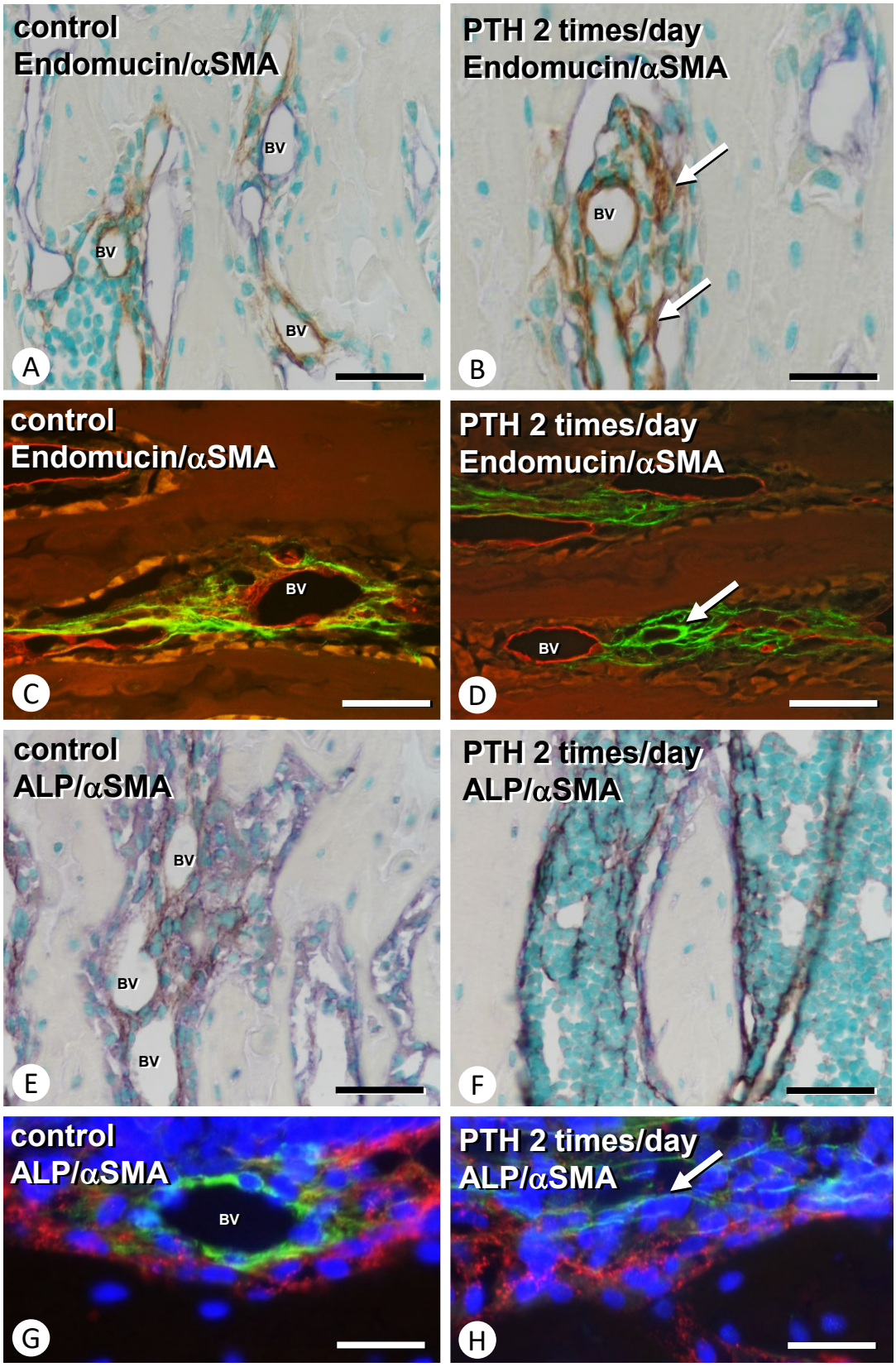
control
Endomucin/αSMA
BV
BV
BV
A
PTH 2 times/day
Endomucin/αSMA
BV
B
control
Endomucin/αSMA
BV
C
PTH 2 times/day
Endomucin/αSMA
BV
D
control
ALP/αSMA
BV
BV
BV
E
PTH 2 times/day
ALP/αSMA
F
control
ALP/αSMA
BV
G
PTH 2 times/day
ALP/αSMA
H

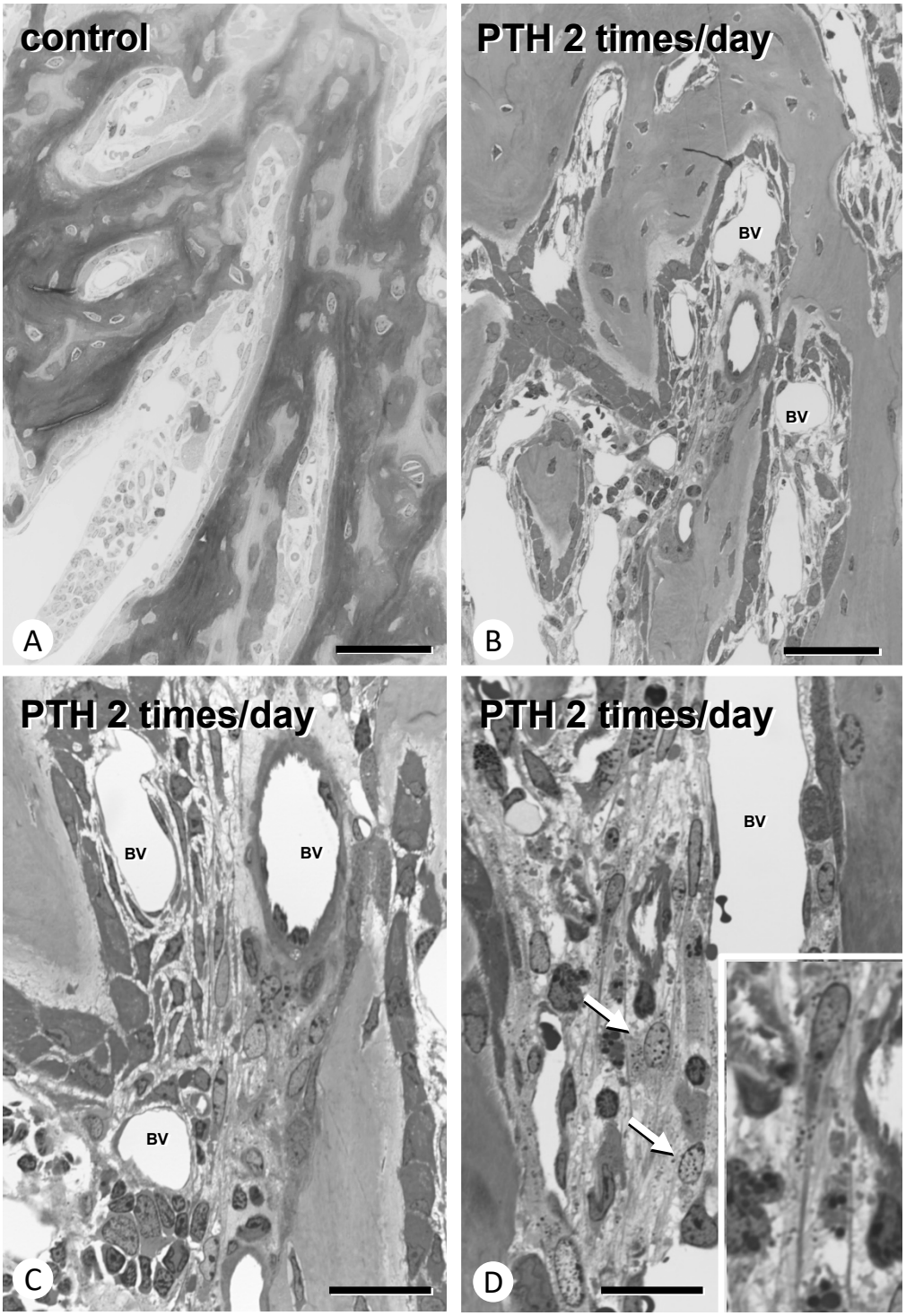
control
A
PTH 2 times/day
BV
BV
B
PTH 2 times/day
BV
BV
BV
C
PTH 2 times/day
BV
D